Site-Directed Mutation Study on Hyperthermostability of Rubredoxin from *Pyrococcus furiosus* Using Molecular Dynamics Simulations in Solution

Dong Hyun Jung, Nam Sook Kang, and Mu Shik Jhon*

Department of Chemistry and Center for Molecular Science, Korea Advanced Institute of Science and Technology, 373-1 Kusung-dong Yusung-gu, Taejon 305-701, Korea

Received: June 18, 1996; In Final Form: September 12, 1996[⊗]

The hyperthermostable protein rubredoxin from *Pyrococcus furiosus* is a 53-residue protein with a three-stranded antiparallel β-sheet and several loops. In this paper, the hydrophobic interaction of residues on the surface of the protein was investigated as well as electrostatic interactions between residues. To investigate the effect of changes of electrostatic and hydrophobic interactions on the structure and the dynamic property of *P. furiosus* rebredoxin, molecular dynamics simulations in solution were performed on three mesophilic rubredoxins, *P. furiosus* rubredoxin, and five mutants of *P. furiosus* rubredoxin. Glu 14 of *P. furiosus* has a backbone hydrogen bond with N-terminal and multiple electrostatic interactions with Ala 1, Trp 3, and Phe 29. The multiple electrostatic interactions make the residues around the N-terminal stable, and the hydrogen bond between Glu 14 and Ala 1 remains even at high temperature. The flexibility of a loop from Asp 15 to Gly 26 is reduced by making the loop closer to the main part of rubredoxin by virtue of the multiple electrostatic interactions of Glu 14. In the middle of the β-sheet, three hydrophobic residues, Val 4, Ile 11, and Leu 51, make the cluster binding the three strands of the β-sheet. This cluster aggregates tightly to stabilize the β-sheet and furthermore the whole protein. These interactions are considered to be important in maintaining the hyperthermostability.

1. Introduction

Proteins display a wide distribution of temperatures at which they undergo thermal denaturation. Even for proteins with the same biological function, the denaturation temperatures differ from each other depending on the natural range of temperature experienced by the organisms producing the proteins. The variety in protein thermostability has attracted considerable scientific interest from medicine and industry. The protein folding mechanism has also been studied, closely related to the thermostability. Many workers have made efforts to discover the molecular basis of the protein thermostability, only to come to the pessimistic conclusion that the origin of thermal stability remains obscure.

In a number of globular proteins, their stability seems to be due not to a fundamental difference in structures of the protein but to the combination of many small interactions in a protein. These interactions, which involve hydrogen bonds, salt bridges between charged groups, dipole−dipole interactions, disulfide bonds, and hydrophobic interactions, have been discussed as stabilizing factors that maintain the native structure of proteins.[1−4] In addition to the discussions about interactions in proteins, mutation studies have proven to be an effective approach for the investigation of the protein thermostability. Even one residue replacement on a protein sequence can influence the protein thermostability, although its effects are generally quite small.[4−8] However, in spite of many efforts, there has not been any generally accepted principle which can account for increasing protein thermostability until now.

Organisms exhibiting optimal growth temperatures as high as 105 °C have been identified.[9−11] Proteins from these organisms can maintain their stability to temperatures at which most mesophilic proteins denature. *Pyrococcus furiosus* is a hyperthermophile isolated by Fiala and Stetter[10] from the vicinity of a Mediterranean volcanic vent. This microorganism grows under anaerobic conditions and has an optimal growth temperature of 100 °C. The system under consideration in this paper is a small (53 amino acids) non-heme iron protein rubredoxin from *Pyrococcus furiosus* (RdPf). It was sequenced in 1991,[12] and X-ray crystallographic studies on both its oxidized and reduced forms have been done.[13] An NMR solution structure was resolved for the Zn-substituted RdPf.[14] The structures from X-ray and NMR studies are very similar and show common interactions which are considered to be important for stability.[15] The overall structure of RdPf obtained from X-ray crystallography is similar to the structures of mesophilic rubredoxins. All rubredoxins are basically composed of a three-stranded antiparallel β-sheet, several loops, a tetrahedral array of four cystein sulfur atoms ligating a single iron atom, and a hydrophobic core.[13] The structural differences of RdPf from mesophilic rubredoxins in X-ray crystal structure are a more extensive backbone hydrogen-bonding network in the β-sheet and multiple electrostatic interactions of the Glu 14 side chain with three other residues (the N-terminal nitrogen of Ala 1, the indole nitrogen of Trp 3, and the amide nitrogen group of Phe 29) (see Figure 1a).[13] It is especially emphasized that the N-terminal has a backbone hydrogen bond with Glu 14. This hydrogen bond is not present in mesophilic rubredoxins. The thermostability of the protein is thought to be related to the presence of the hydrogen bond at the N-terminal.[13,14,16] In a recent pH dependence experiment using a variety of spectroscopic methods, it was found that the electrostatic interactions of charged residues on the protein surface have an important role in maintaining RdPf's conformation to such a high temperature as 100 °C.[17] Another protein, aldehyde ferredoxin oxidoreductase from *P. furiosus*, also shows hyperthermostability. In this protein, there are more electrostatic interaction pairs than in its mesophilic counterparts, and they have also been suggested as a major factor causing increased protein

* To whom all correspondence should be addressed. e-mail: jwater@sorak.kaist.ac.kr.

[⊗] Abstract published in *Advance ACS Abstracts,* December 15, 1996.

S1089-5639(96)01794-X CCC: $14.00

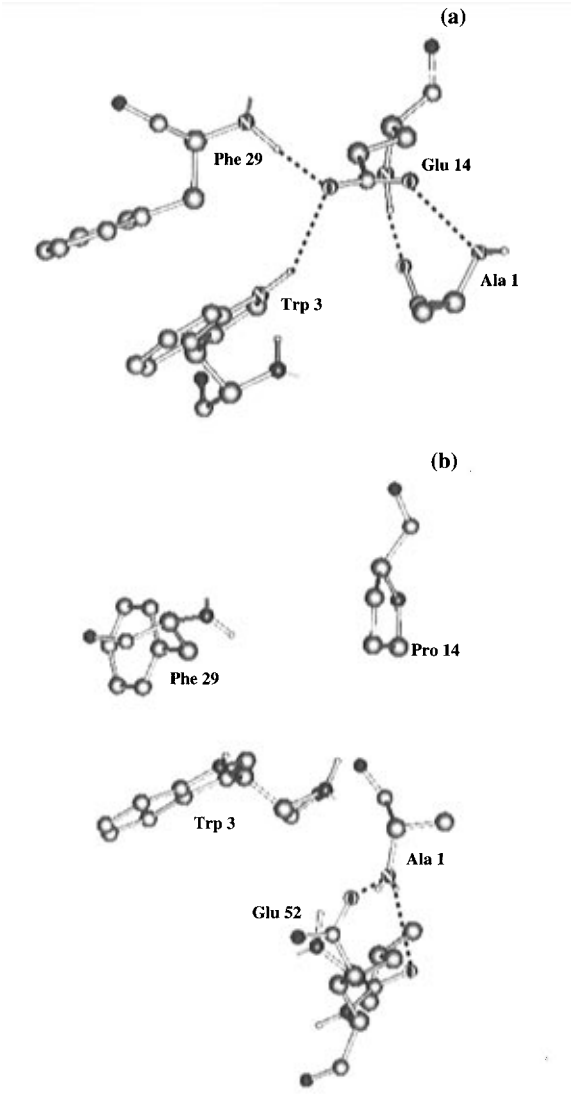

Figure 1. Conformation around the N-terminal in (a) wild RdPf and (b) mutant Glu 14→Pro.

thermostability.[18] These approaches cannot, however, give detailed information about the molecular basis of thermostability, although the hint of thermostability was obtained from those considerations.

In order to investigate the effects of amino acid sequence on the structure and dynamic properties at the molecular level, molecular dynamics simulations for wild RdPf and logically designed five mutants were conducted in solution. Before these mutation studies, it was necessary to compare the behavior of RdPf in solution with that of mesophilic rubredoxins from *Desulfovibrio gigas* (RdDg), *Clostridium pasteurianum* (RdCp), and *Desulfovibrio vulgaris* (RdDv). For comparison, we carried out molecular dynamics simulations on four rubredoxins in solution at 298 and 373 K.

2. Methods of Calculation

At first, for the comparative study we calculated the four simulation systems—RdPf and three mesophilic rubredoxins, RdDg, RdCp and RdDv—in solution at 298 and 373 K. Next, for the mutation study the calculations were carried out on RdPf wild type and five one-site mutated mutants. In all systems, the C-terminal and N-terminal were varied to uncharged forms, $-COO^- \rightarrow -COOH$ and $-NH_3^+ \rightarrow -NH_2$. All simulations were done using the CHARMM program modified for use on the SGI INDIGO workstation (versions 22.0 and 23.0).[19] The resulting compatibility between two versions was validated. CHARMM 23.0 united atom parameters were used for all atoms including the iron in the rubredoxin. All interactions were calculated between pairs of atoms closer than 9.5 Å. Trajectories were calculated using the Verlet algorithm with a time step of 1 fs. A shifted function was employed to smoothly reduce the energies and to avoid discontinuities in the energies and their derivatives for the van der Waals term and electrostatic term. In solution simulation, the dimensions of the water box were $43.4 \times 37.2 \times 34.1$ Å^3 and the periodic boundary condition was applied. The initial simulation structures were taken from X-ray structures[13,20−22] from the Brookhaven Protein Data Bank, and the mutated structures were produced by the CHARMM program. Before molecular dynamics simulations, they were relaxed sufficiently by "steepest descent minimization" to eliminate the initial strains in systems. Heating from 0 K to simulation temperature (298 or 373 K) for 10 ps and following the equilibration of 10 ps at the target temperature were done. Product simulations were done in 30 ps, and the data from the last 10 ps were analyzed.

3. Results and Discussion

The sequence specificity is the main subject to be discussed in this study and was investigated by site-directed mutations using molecular dynamics simulations. We analyzed the interaction energy of important residues and dynamic properties of the system for the discussion of protein stability. The interaction energies of residues were calculated on the basis of the mean structure of each protein obtained by averaging the coordinate sets collected at 0.5 ps intervals during last 10 ps of a 30 ps product simulation. A more detailed analysis of dynamic variability was made through the root-mean-square (rms) fluctuation of each residue in the protein. The rms fluctuation was obtained by comparing the each mean structure with the collected coordinate sets.

3.1. Comparison between RdPf, RdDv, RdCp, and RdDg at 298 and 373 K. The dynamics of RdPf and three mesophilic rubredoxins, RdDv, RdCp, and RdDg, were studied to prepare the reference for the comparison of dynamic behavior of wild type RdPf and mutants. These simulations were carried out at 298 and 373 K. From the results of the simulations, averaged energies, hydrogen bonds lists, and rms fluctuations of four rubredoxins at 298 and 373 K were analyzed. Although the direct comparison of the absolute value of energies between different animo acid sequences is meaningless, it is possible to understand the stability through the comparison of energy difference for each system with respect to the temperature increase. From the averaged energy data displayed in Table 1, we know that by increasing the temperature from 298 to 373 K the electrostatic energy of RdPf is less destabilized than that of mesophilic rubredoxins. This stability of electrostatic energy is of advantage to the stability of the protein as reported by Cavagnero *et al.*[17] However, this result cannot give us a detailed molecular scale reason for the stability of protein. Hence, we need to investigate each intra- and intermolecular interaction. The rms fluctuation data in Figure 2 indicate dynamic property differences between RdPf and mesophilic rubredoxins. RdPf has a similar fluctuation pattern at 298 and 373 K. However, in mesophilic rubredoxins at 373 K, large deviations from the fluctuation shown at 298 K occur at the N-terminal and at residues 15−26. In RdPf, hydrogen bonds list obtained from an averaged coordinate contains the backbone hydrogen bond between Glu 14 and Ala 1, even at 373 K. (Position 2 in mesophilic rubredoxins corresponds to position 1 in RdPf due to the lack of an N-terminal methionine residue in RdPf. All

TABLE 1: Averaged Total, van der Waals, and Electrostatic Energies (in kcal/mol) of RdPf, RdCp, RdDv, and RdDg

rubredoxin	E_{total} (298 K)	E_{VDW} (298 K)	E_{elec} (298 K)	E_{total} ($\Delta E/\|E\|$)[a] (373 K)	E_{VDW} ($\Delta E/\|E\|$) (373 K)	E_{elec} ($\Delta E/\|E\|$) (373 K)
RdPf	−16 867.0	1219.1	−18 910.0	−14 997.4 (0.11)	1049.0 (−0.14)	−18 537.1 (0.020)
RdCp	−16 495.6	1126.6	−18 537.1	−14 483.8 (0.12)	948.5 (−0.16)	−17 377.7 (0.063)
RdDv	−16 554.2	1238.1	−18 561.5	−14 389.5 (0.13)	1058.7 (−0.14)	−17 362.3 (0.065)
RdDg	−16 582.7	1216.0	−18 630.0	−14 376.1 (0.13)	1032.6 (−0.15)	−17 339.0 (0.069)

[a] $\Delta E/|E| = (E^{373\ K} - E^{298\ K})/|E^{298\ K}|$. The negative value of this quantity means that the energy is lowered with increasing temperature.

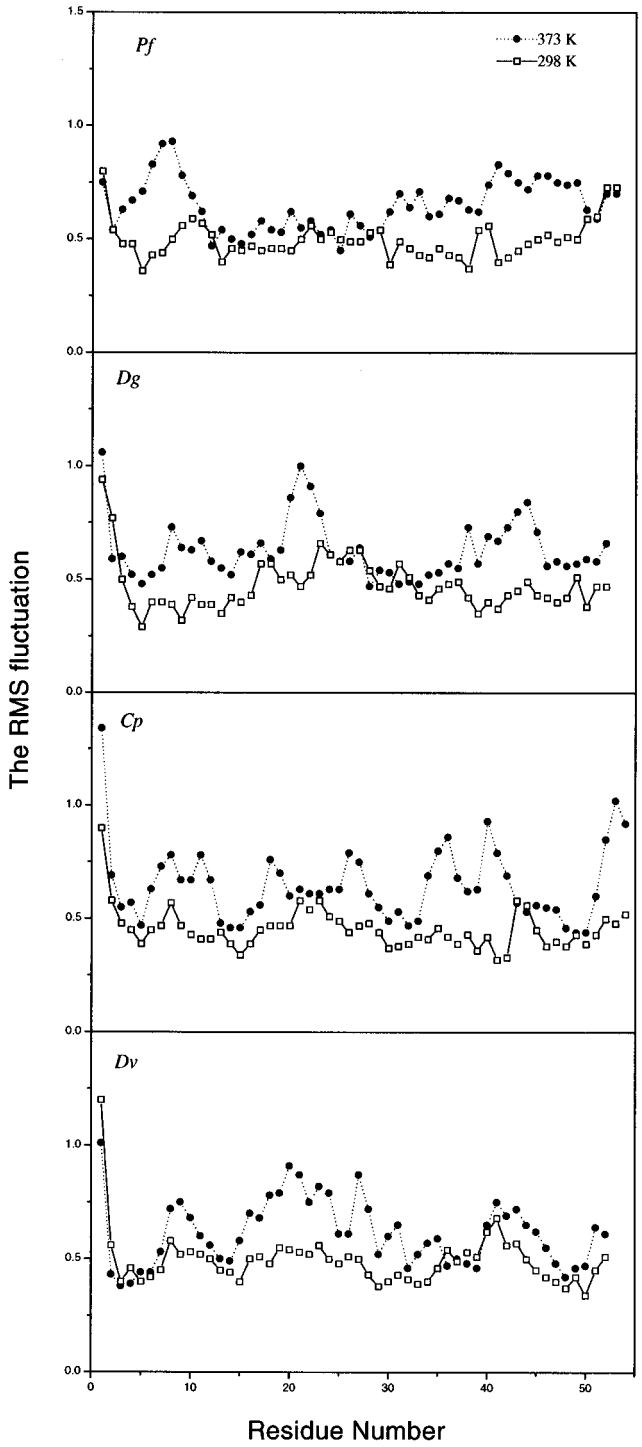

Figure 2. The rms fluctuation of RdPf, RdDg, RdCp, and RdDv at 298 and 373 K.

residue numbers in this paper correspond to the RdPf sequence, except in Figure 2.) The energy of the hydrogen bond, −2.544 kcal/mol, is calculated from the mean structure, and this energy is lower than the reference, −2.25 kcal/mol, used as the definition of a hydrogen bond in the TIP3P water model.[23] Other mesophilic rubredoxins have a Pro residue at the 14 position so that they do not have a hydrogen bond at the N-terminal. This hydrogen bond is one of the characteristics of RdPf. We will discuss these structural and dynamic properties in more detail.

3.2. Effects of Electrostatic Interactions of Glu 14. 3.2.1. Mutation of Glu 14 to Pro. As explained before, RdPf has a three-stranded antiparallel β-sheet starting from the N-terminal; i.e., the β-sheet has a hydrogen bond at the N-terminal. The fact that the β-sheet includes the N-terminal is one of the differences from mesophilic rubredoxins. In the sequence around this region, RdPf has Glu 14 instead of Pro, which is prevalent at that position in most mesophilic rubredoxins with the exception of *Megasphaera elsdenii* rebredoxin (RdMe).[24] Ala 1 is also a characteristic residue, but Glu 14 has more electrostatic interactions with other residues to help the backbone hydrogen bond of the N-terminal to be stable at higher temperature, which are thought to be important for maintaining the thermal stability of RdPf.[13] Figure 1a shows the multiple electrostatic interactions of the Glu 14 side chain. The energies of the interactions with Ala 1, Trp 3, and Phe 29 are calculated as −15.44, −4.12, and −6.50 kcal/mol, respectively. This is the reason why Glu 14 was chosen as the first target for mutation. By mutating Glu 14, we intended to eliminate the backbone hydrogen bond at the N-terminal and multiple electrostatic interactions of Glu 14. To do this, Glu 14 was replaced by Pro. In the mean structure of mutant Glu 14→Pro, the hydrogen bond network in the β-sheet remains in the original state, except that the hydrogen bond between Glu 14 and Ala 1 in wild type RdPf disappears; the distance of Pro 14 N to Ala 1 O is 5.61 Å. The disappearance of the hydrogen bond at the N-terminal is natural because Pro has no amide proton. The conformational changes of the four residues Ala 1, Trp 3, Pro 14, and Phe 29 are shown in Figure 1b. The amino nitrogen of Ala 1 is totally inverted to direct to the C-terminal. A comparison between parts a and b of Figure 1 shows that the side chain of Glu 14 holds the amino nitrogen of Ala 1, making a main chain to main chain hydrogen bond possible.

Investigation of changes in rms fluctuation patterns of mutant Glu 14→Pro reveals the prominent change occurs at residues 15−26 which form a loop (see Figure 3). This pattern is a common feature of rms fluctuations of the mesophilic rubredoxins RdCp, RdDg, and RdDv at high temperature (see Figure 2). This increase in rms fluctuation of the loop seems to be related to the structural changes of protein with increasing temperature. To obtain information about the structural changes in the region of the loop due to the mutation of Glu 14 to Pro, we measured the angle θ formed by two lines; one is the crosscut of two least-squares planes passing through Cα's from 1 to 14 (plane 1) and from 15 to 26 (plane 2), and the other is the projected image of the axis of β-sheet on plane 1 (see Figure 4). The angle θ of mesophilic rubredoxins increases with increasing temperature, while that of RdPf decreases (see Table 2). The measurement of θ in mutant Glu 14→Pro, Pro 14 of which has no electrostatic interactions with any other residues, indicates the loop is relatively separate from the main part of the protein. The value of θ is related to the rms fluctuation of

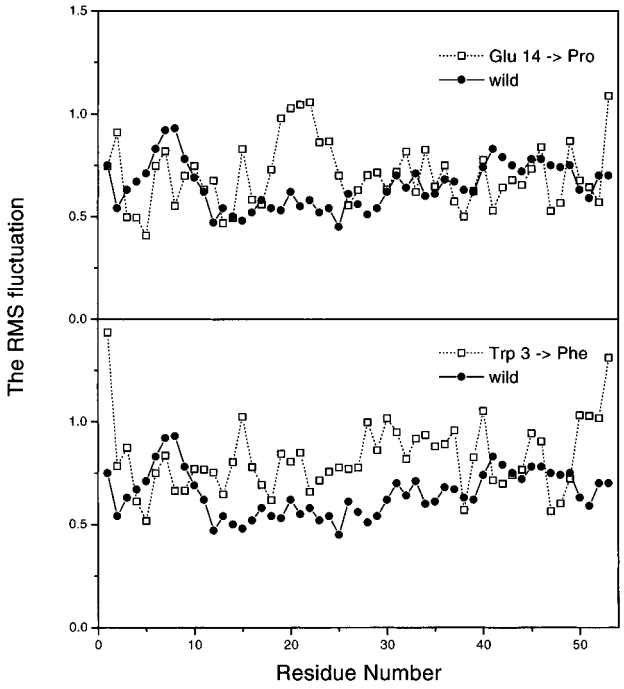

Figure 3. The rms fluctuation plots of mutants Glu 14→Pro and Trp 3→Phe at 373 K.

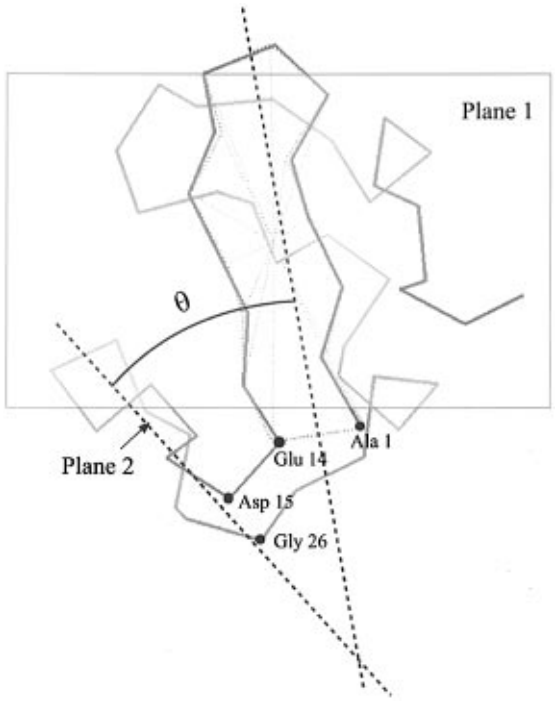

Figure 4. The angle θ made by two lines.

TABLE 2: Angle θ Calculated in Each System

	θ (deg)			θ (deg)	
rubredoxin	298K	373K	rubredoxin	298K	373K
wild RdPf	30.77	22.90	RdDg	19.62	37.89
RdDv	31.54	39.55	Glu 14→Pro		34.17
RdCp	22.89	43.69	Trp 3→Phe		30.38

the loop as shown in the rms fluctuation plots (see Figures 2 and 3). As explained above, while the rms fluctuation of the loop in wild RdPf shows no difference at 298 and 373 K, in three mesophilic rubredoxins and mutant Glu 14→Pro, a certain increase of rms fluctuation in the loop region exists as temperature rises. This result demonstrates the flexibility of the loop is dependent on the distance between the loop and the main part of the protein, that is, the closer to the main part of the protein the loop becomes, the less flexible it is. We expected the rms fluctuation of Pro 14 in mutant Glu 14→Pro would increase as the interactions of Glu 14 disappeared, but the rms fluctuation of mutant Glu 14→Pro did not show the expected increase at position 14 although the electrostatic interactions certainly disappeared. The stable motion of Pro 14 seems to be based on the conformational rigidity of Pro and the hydrophobic interaction of Pro with phenyl ring of Tyr 12.

3.2.2. Mutation of Trp 3 to Phe. We have mentioned that the side chain of Glu 14 is important for maintaining the N-terminal hydrogen bond by holding the amino group of Ala 1. In addition, the side chain of Glu 14 has electrostatic interactions with other two residues Trp 3 and Phe 29 as well as Ala 1. To investigate the role of the interactions of Glu 14 in detail, another mutation was needed. There is one mesophilic rubredoxin from RdMe with Glu at the position 14. RdMe has Tyr in behalf of Trp at position 3. Glu 14 in RdPf makes a salt bridge with the indole nitrogen of Trp 3. Hence, we selected Trp 3 as a next target to affect the salt bridge. Tyr has a hydroxyl group on the side chain which can make a hydrogen bond, so that we mutated Trp 3 to Phe to ensure the absence of electrostatic interaction with Glu 14 though RdMe has Tyr at position 3. In averaged structure obtained from a simulation, the hydrogen bond network of this mutant shows the hydrogen bond at the N-terminal is not present; the distance of Glu 14 N to Ala 1 O is 4.72 Å, which is too long to make a hydrogen bond but shorter than in the case of mutant Glu 14→Pro. This implies that the multiple electrostatic interactions of Glu 14 with all three residues make the hydrogen bond between Ala 1 and Glu 14 stable.

When the rms fluctuation of mutant Trp 3→Phe (see Figure 3) is compared with that of wild type RdPf, the increases of fluctuation of Ala 1, Phe 3, Glu 14, and Phe 29 are observed, as well as the slight increase in the region of the loop from 15 to 26. The angle θ measures 30.38°, which is between the values obtained in wild RdPf and mutant Glu 14→Pro (see Table 2). The absence of one salt bridge between Glu 14 and Trp 3 makes the loop have in-between stability. From this data, we know that the electrostatic interactions of the Glu 14 side chain with all three residues Ala 1, Trp 3, and Phe 29 have a role in stabilizing the residues around the N-terminal and do not allow the loop starting from 15 and reaching 26 to be free.

3.3. Effect of Hydrophobic Interaction. The hydrophobic interaction has an important role in the conformational stability of proteins. The hydrophobic core in a protein is a particularly essential part since the secondary structure such as the β-sheet is supported on it. RdPf has a hydrophobic core composed of Trp 3, Tyr 10, Tyr 12, Phe 29, Leu 32, Trp 36, and Phe 48. The β-sheet in RdPf is seated on the hydrophobic core. Trp 3, Tyr 10, Tyr 12, and Phe 48 belong to the β-sheet as well as the hydrophobic core. However, mesophilic rubredoxins have almost the same hydrophobic core components. Thus, we cannot find any residue for substitution in the hydrophobic core except Trp 3, the mutation study of which was considered above in detail. On the surface of RdPf, the hydrophobic residues Val 4, Tyr 10, Ile 11, Val 37, Pro 39, Ile 40, Pro 44, and Leu 51 make a beltlike structure around the entire molecule.[16] These residues form hydrophobic clusters around the iron−sulfur complex. One of these clusters is on the β-sheet. In the middle of the β-sheet, there are three hydrophobic residues, Val 4, Ile 11, and Leu 51 (see Figure 5). In mesophilic rubredoxins, a hydrophilic residue is present at one of those three positions.[13] Leu 51 is peculiar to RdPf, but since what we are interested in

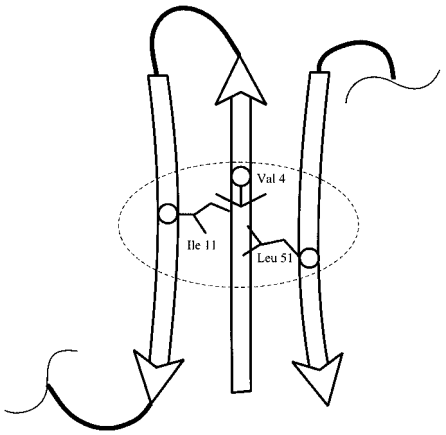

Figure 5. "Hairpin" structure on the β-sheet in wild RdPf. The three residues Val 4, Ile 11, and Leu 51, function as if they are a hairpin tying up three strands of the β-sheet.

is the effect of the three hydrophobic residues on the β-sheet, we selected Ile 11 near N-terminal (we have noticed N-terminal as an important part in the β-sheet) rather than Leu 51.

Ile 11 was replaced with the three residues Ala, Phe, and Glu. Glu exists at position 11 in RdDg and RdDv. Ala and Phe are hypdrophobic residues while Glu is a hydrophilic residue. Ala is smaller and Phe is larger than Ile. The rms fluctuations of the two mutants Ile 11→Ala and Ile 11→Phe show small difference from that of wild type RdPf (see Figure 6). The dynamic behavior of the mutant Ile 11→Phe appears to be more stable than that of the wild type. In particular, the fluctuation of the hydrophobic residues, Tyr 10 and Tyr 12, is almost identical to that of the wild type. The rms fluctuation pattern of the Glu-substituted mutant has a very different thermal motion overall (see Figure 6). The rms fluctuation of Tyr 10, Glu 11, and Tyr 12 in the mutant Ile 11→Glu is about twice as large as those of Tyr 10, Ile 11, and Tyr 12 in the wild type. Tyr 10 and Tyr 12 are components of the hydrophobic core. The fluctuation of other core residues, therefore, is also increased as these two core residues are made more flexible. These destabilized core residues can affect the stability of protein as a whole. This means that protein stability is much influenced by a mutation altering position 11 to hydrophilic residue Glu.

The hydrophilicity of Glu 11 residue in mutant Ile 11→Glu can be represented by the interaction of Glu 11 with water molecules in the first hydration shell around Val 4, Glu 11, and Leu 51. To investigate the solvent effect, the water molecules 3.5 Å from each of the three residues were counted, and the surface area of the three residues was calculated for wild RdPf and mutants Ile 11→Ala, Ile 11→Phe, and Ile 11→Glu. To obtain information about the orientational structure of the hydration shell, orientations of water molecules were investigated using the dipole directions of the hydration water molecules. The z axis of the water molecule is defined as the vector direction opposite to the electric dipole moment of the water molecule. Table 3 presents results for the hydration shell water molecules. The ratio $N_{\theta z>90°}/N_{\theta z<90°}$, the number of water molecules with $\theta_z > 90°$ to that with $\theta_z < 90°$, means the extent to which the water molecules in the first shell are oriented in such a way that the water O−H bond points radially outward from the cluster which contains the three residues at positions 4, 11, and 51:

$$\cos \theta_z = \boldsymbol{\mu}_{ccO} \cdot \boldsymbol{\mu}_z$$

where $\boldsymbol{\mu}_z$ is the unit vector in z direction,

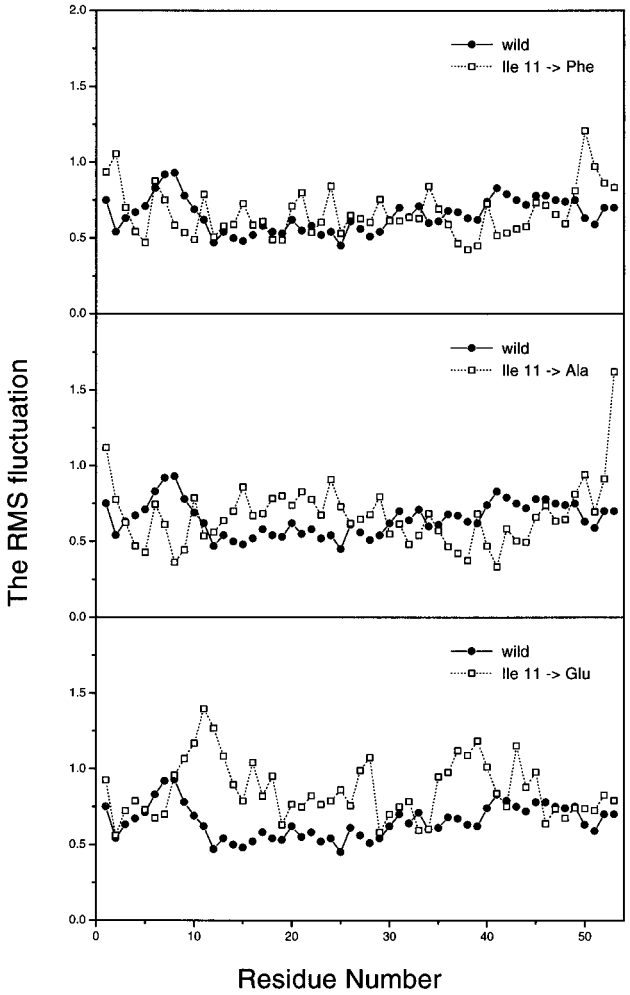

Figure 6. The rms fluctuation plots of mutants Ile 11→Ala, Ile 11→Phe, and Ile 11→Glu at 373 K.

TABLE 3: Information about Water Molecules in First Hydration Shell of 4, 11, and 51 Residues

system	SASA (Å^2)[a]	no. of water molecules	$N_{\theta z>90°}/N_{\theta z<90°}$
wild RdPf	742.65	21	0.476
Ile 11→Ala	719.43	21	0.619
Ile 11→Phe	786.28	31	0.613
Ile 11→Glu	767.60	29	0.276

[a] This solvent accessible surface area (SASA) is calculated for three residues at position 4, 11, and 51.

$$\boldsymbol{\mu}_{ccO} = (\mathbf{r}_{cc} - \mathbf{r}_O)/|\,\mathbf{r}_{cc} - \mathbf{r}_O\,|$$

$\mathbf{r}_{cc}$ is the vector to center of mass of the cluster. In wild RdPf, mutant Ile 11→Ala, and mutant Ile 11→Phe, about half or more of the water molecules point radially outward. This fact show the hydrophobicity of Ile 11, Ala 11, and Phe 11. In mutant Ile 11→Glu, most of water molecules in the first shell around Val 4, Glu 11, and Leu 51 point radially inward (see Table 3). In contrast to the cases of hydrophobic residues at position 11, Glu 11 attracts the O−H bonds of water molecules to create a stronger interaction between Glu 11 and the water molecule. This solvent interaction with Glu 11 prevents Glu 11 from aggregating easily with Val 4 and Leu 51. Thus, the thermostability of the β-sheet and the protein is increased by the hydrophobic interaction of three residues on the β-sheet. These aggregate more tightly with temperature[25] to bind the three strands of the β-sheet as if they were a "hairpin" (see Figure 5). In the case of mutant Ile 11→Glu, the cluster is not expanded on the 9−14 strand, and the "hairpin" structure is

broken because Glu 11 does not take part in the cluster. The hydrophobic interaction energy part is not yet implemented in potential function perfectly. Thus, the real effect of the hydrophobic interaction on the thermostability may be stronger than the simulation results suggest.

4. Conclusion

We have investigated the effect of electrostatic and hydrophobic interactions on the stability of protein RdPf. When we compared RdPf with mesophilic rubredoxins, fundamental differences in structural elements were not found. More plain interactions in the protein than mesophilic rubredoxins are suggested as the main cause of hyperthermostability. We paid particular attention to the multiple electrostatic interactions of Glu 14 with three residues, Ala 1, Trp 3, and Phe 29. These interactions are thought to be important in the stabilization of the hydrogen bond at the N-terminal. It was found that the side chain of Glu 14 holds the amino nitrogen of Ala 1 to make the hydrogen bond at the N-terminal possible by having the amide oxygen of Ala 1 directed toward the amide proton of Glu 14. This stabilizing effect is believed to account for the hyperthermostability of RdPf. The flexibility of a loop from 15 to 26 is influenced by the relative compactness of the protein. The electrostatic interactions of Glu 14 have the loop be closer to the main part so that compactness is increased, which has an important role in stabilizing RdPf. In the middle of the β-sheet, there are three hydrophobic residues, Val 4, Ile 11, and Leu 51, aggregating together due to hydrophobic interaction. This hydrophobic cluster on the β-sheet is peculiar to RdPf. The cluster aggregates tightly to hold the strands of the β-sheet as if they were a "hairpin" so that the three strands of the β-sheet can maintain their conformation.

Acknowledgment. This work was supported in part by the Korea Research Center for Theoretical Physics and Chemistry.

References and Notes

(1) Straume, M.; Murphy, K. P.; Freire, E. *Biocatalysts at Extreme Temperatures*; American Chemical Society: Washington, DC, 1992; Chapter 9.
(2) Lim, W. A.; Sauer, R. T. *J. Mol. Biol.* **1991**, *219*, 359.
(3) Murphy, K. P.; Privalov, P. L.; Gill, S. J. *Science* **1990**, *247*, 559.
(4) Nicholson, H.; Becktel, W. J.; Matthews, B. W. *Nature* **1988**, *336*, 651.
(5) Matthews, B. W.; Nicholson, H.; Becktel, W. J. *Proc. Natl. Acad. Sci. U.S.A.* **1987**, *84*, 6663.
(6) Menendez-Arias, L.; Argos, P. *J. Mol. Biol.* **1989**, *206*, 397.
(7) Pakula, A. A.; Sauer, R. T. *Nature* **1990**, *344*, 363.
(8) Kwon, K.-S.; Kim, J.; Shin, H. S.; Yu, M.-H. *J. Biol. Chem.* **1994**, *269*, 9627.
(9) Stetter, K. O. *Nature* **1982**, *300*, 258.
(10) Fiala, G.; Stetter, K. O. *Arch. Microbiol.* **1986**, *145*, 56.
(11) Stetter, K. O.; Lauerer, G.; Thomm, M.; Neurer, A. *Science* **1987**, *236*, 822.
(12) Blake, P. R.; Park, J.-B.; Bryant, F. O.; Aono, S.; Magnuson, J. K.; Eccleston, E.; Howard, J. B.; Summers, M. F.; Adams, M. W. W. *Biochemistry* **1991**, *30*, 10885.
(13) Day, M. W.; Hsu, B. T.; Joshua-Tor, L.; Park, J.-B.; Zhou, Z. H.; Adams, M. W. W.; Rees, D. C. *Protein Sci.* **1992**, *1*, 1494.
(14) Blake, P. R.; Park, J.-B.; Zhou, Z. H.; Hare, D. R.; Adams, M. W. W.; Summers, M. F. *Protein Sci.* **1992**, *1*, 1508.
(15) Blake, P. R.; Day, M. W.; Hsu, B. T.; Joshua-Tor, L.; Park, J.-B.; Hare, D. R.; Adams, M. W. W.; Rees, D. C.; Summers, M. F. *Protein Sci.* **1992**, *1*, 1522.
(16) Bradley, E. A.; Stewart, D. E.; Adams, M. W. W.; Wampler, J. E. *Protein Sci.* **1993**, *2*, 650.
(17) Cavagnero, S.; Zhou, Z. H.; Adams, M. W. W.; Chan, S. I. *Biochemistry* **1995**, *34*, 9865.
(18) Chan, M. K.; Mukund, S.; Kletzin, A.; Adams, M. W. W.; Rees, D. C. *Science* **1995**, *267*, 1463.
(19) Brooks, B. R.; Bruccoleri, R. E.; Olafson, B. D.; States, D. J.; Swaminathan, S.; Karplus, M. *J. Comput. Chem.* **1983**, *4*, 187.
(20) Watenpaugh, K. D.; Sieker, L. C.; Jensen, L. H. *J. Mol. Biol.* **1980**, *138*, 615.
(21) Adman, E. T.; Sieker, L. C.; Jensen, L. H. *J. Mol. Biol.* **1991**, *217*, 337.
(22) Frey, M.; Sieker, L. C.; Payan, F. *J. Mol. Biol.* **1987**, *197*, 525.
(23) Jorgensen, W. L.; Chandrasekhar, J.; Madura, J. D.; Impey, R. W.; Klein, M. L. *J. Chem. Phys.* **1983**, *79*, 926.
(24) Bachmeyer, H.; Yasunobo, K. T.; Peel, J. L.; Mayhew, S. *J. Biol. Chem.* **1968**, *243*, 1022.
(25) Ben-Naim, A. *Hydrophobic Interactions*; Plenum: New York, 1980; Chapter 5.